Proceedings of the 17th World Congress
The International Federation of Automatic Control
Seoul, Korea, July 6-11, 2008

A Mechatronic Approach for Anti-slip Control in Railway Traction

T X Mei*‡ J H Yu*, D A Wilson*

** School of Electronic and Electrical Engineering, The University of Leeds, Leeds LS2 9JT, UK (‡Tel: 44 113 3432066; e-mail: t.x.mei@leeds.ac.uk).*

Abstract: This paper presents a novel mechatronic approach for the detection of wheel slip/slide and anti-slip control in railway traction systems, to enable an optimal use of adhesion in poor contact conditions. The proposed technique explores the variations in wheelset dynamic properties caused by condition changes at the wheel-rail contact and detects slip conditions from the torsional resonant vibrations of the wheelset axle indirectly. The modeling of a typical traction system, consisting of an induction traction motor (with associated power inverter and field-orientated control) connected to a wheelset via a gearbox, is introduced. The development of the slip detection and control scheme is presented, and the effectiveness of the proposed technique is demonstrated using computer simulations.

1. INTRODUCTION

Railway traction is a complex mechatronic system, as the traction motors and the associated controls have to work in harmony with the complex mechanical loads especially at the wheel-rail interface. Wheel slip/slide occurs when applied tractive effort exceeds the level of maximum adhesion available at the wheel-rail interface, e.g. in poor weather conditions or with contaminated tracks. Apart from the potential impact on normal operations of a rail network, the wheel slip/slide causes undesirable wear to both wheel/track surfaces and increases the requirements/costs of maintenance. Most conventional wheel slip protection schemes involve measures to limit the amount of slip ratio (relative speed between a wheel and the train) to a set value that is sometimes necessary to be tuned on line, and in more extreme cases to control the wheel rotational acceleration below a pre-defined threshold [Park et al, 2001; Schwartz et al, 1997; Watanabe et al, 1997; and Yasuoka et al, 1997]. The performance of those schemes is affected by the limited accuracy of the encoders used in the traction systems, which is typically less than 100 pulses per revolution, as well as difficulties related to a reliable measurement of vehicle absolute speed in slip/slide conditions.

Furthermore, the wheel-rail contact characteristics are subject to large variations, and it is difficult to ensure optimal use of the available adhesion because there is no fixed relationship between the slip ratio and the maximum adhesion. There have been studies on the use of so-called disturbance observers to detect the longitudinal creep forces and hence to derive the rate of change on the slip curve [Kadowaki, et al., 2002; Kim, et al., 1999] with the aim to optimise the control of slip ratio. However there seems to be little reported on the practicality and effectiveness of the approach.

Additional measures may be used to improve the adhesion level at the wheel-rail interface. The use of sand machines, often installed on locomotives, has been for many years a popular and effective means to increase the traction. More recently specially formulated chemicals (friction modifiers) are reported to have the effect of adhesion enhancement, although some tests have produced results that are less supportive [McEwen, 2003; and Waring, 1994]. At the system (infrastructure) level, it is also possible to improve the track conditions, e.g. by removing the contaminations, although currently known techniques are in general expensive and/or impractical for implementation.

This study investigates an indirect approach for the wheel slip detection which explores how the wheelset dynamics are affected by changes in contact conditions. The study demonstrates how the torsional mode of a conventional solid axle wheelset may be linked to the wheel slip/slide and consequently proposes a novel technique to detect wheel slip by identifying the variations in wheelset torsional vibrations. There is no need for the measurement of slip ratio and/or estimation of creep forces at the wheel-rail interface.

Some of the findings have been published previously. A fundamental examination of the concept and the feasibility for real applications was discussed in [Mei et al, 2006], followed by a study on possible control solutions in [Yu et al, 2006]. This study presents the latest results from the research project, in particular the development of practical slip detection and re-adhesion control (to recover from slip conditions) strategies.

The paper is organised as follows. The configuration of the traction system used in the study is presented and mathematical models are provided in section 2. Section 3 describes the fundamental properties of wheel-rail contact forces and gives an analysis on how wheelset dynamic behaviour may be affected by different contact conditions. The development of a novel anti-slip control scheme and performance assessment is presented in section 4, and key conclusions are drawn in section 5.

2. SYSTEM AND MATHEMATICAL MODELS

A standard configuration as illustrated in Fig 1 is used in the study, which involves a conventional solid-axle wheelset connected to an AC traction motor through a traction gearbox. A typical three-phase induction motor is used for the provision of traction for the wheelset and ¼ of a typical vehicle. Connections between the wheelset and the bogie/vehicle in the longitudinal direction are assumed to be solid, as the stiffness is normally very high and the associated dynamics is not of significant relevance to this study.

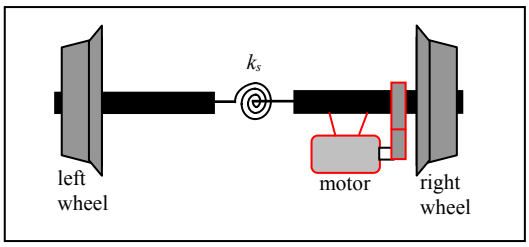

Fig. 1. Wheelset configuration

The spring k_s in Fig. 1 represents the equivalent stiffness for the first torsional mode of the wheelset. The frequency is typically about 60Hz, but can vary between perhaps 40Hz for a soft axle and to around 80Hz for a more rigid one.

An overall diagram of the mathematical models is shown in Fig 2. The models for the induction motor, the power electronics and the associated vector control scheme are fairly standard, some of which are available from SIMULINK SimPower toolbox [Yu et al 2006].

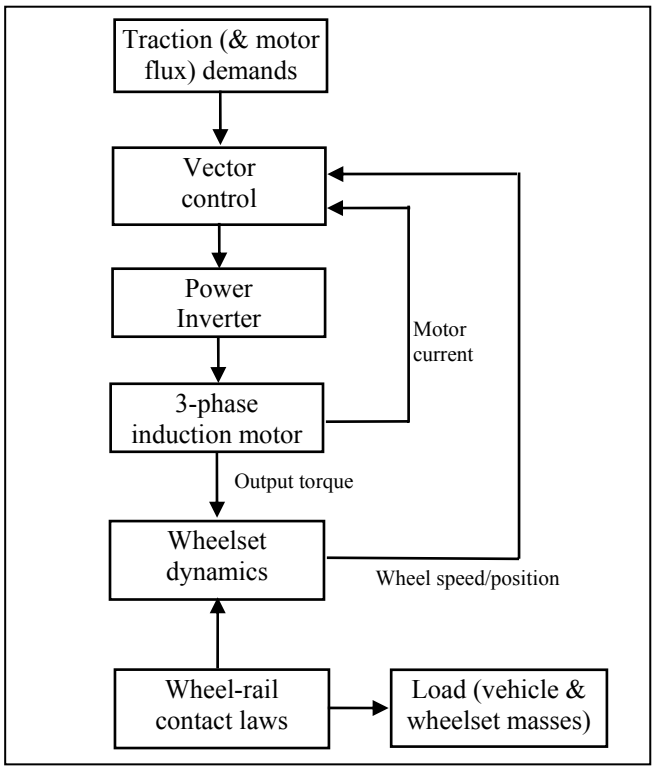

Fig. 2. Block diagram of the system models

However, the mechanical models of the systems are much more complex. One of the key issues is the modelling of the wheel-rail contact forces, as it provides the essential link between the output of the traction motor and the mechanical load. The wheel-rail contact mechanics involves the contact forces caused by so-called creepages between the wheel and rail surfaces which are small relative velocities resulted from elastic deformation of the steel at the point of contact. The overall creep force at the contact point is a non-linear function of the creepage and limited by the available adhesion. Measurements from many experimental studies have indicated that the creep – creep force relations follow a general trend as indicated in Fig. 3 [Polach, 2003]. Typically, a creep – creep force curve can be partitioned into three different sections – the low creep or the linear section (of the initial slope); the large creep or the non-linear section (before the peak point); and the slip or unstable region (beyond the peak point).

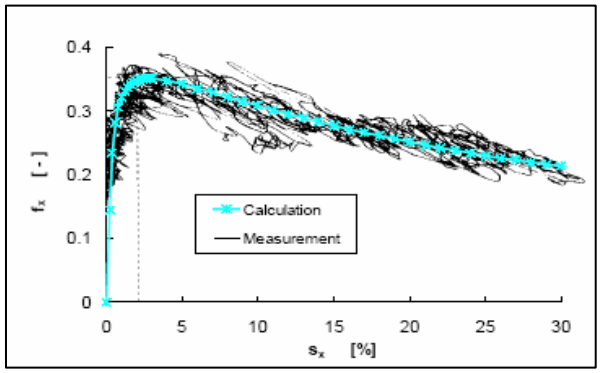

Fig. 3. Creep – creep force curve

Also, the overall contact force at the wheel-rail interface is affected by creepages in both longitudinal and lateral directions. Apart from the creep forces necessary to produce the tractive effort which are in the longitudinal direction only and are largely equal between the two wheels of a powered axle, there are additional creepages due to the wheelset motions (e.g. yaw and lateral) and contact geometries. The longitudinal creep forces of the two wheels of the same wheelset in this case produce a yaw toque but no net traction effort. Because all the creepages are developed at the same contact patch, there will obviously be dynamic interactions and the overall contact force is constrained by the adhesion.

Furthermore, the properties of the curves are subject to large and uncertain variations due to condition changes at the two contacting surfaces, such as contaminations, weather, wheel dynamic loading, and vehicle speed. Not only the maximum adhesion available and the corresponding creepages are difficult to predict, but also the initial slope in the linear region can be seriously affected.

For computer simulations in the study, a number of look-up tables are generated and used to represent different contact conditions. Those are somewhat idealised, but they provide essential features of wheel-rail contact laws [Polach, 2003].

The dynamics of the wheelset axle in the rotational direction should strictly be modelled using a distributed parameter model, but it can be readily demonstrated that the only two dominant modes are necessary to be included in the study – the common rotation of the wheelset (rolling forward) and the first torsional mode between the two wheels. A simplified mechanical model is given in equations 1-4, representing the rotation of the right wheel, rotation of the left wheel and longitudinal motion of the wheelset (and the vehicle).

$$\left(J_w + n^2 J_{mg}\right)\dot{\omega}_R = n \cdot T_e - T_{tor} - r_R \cdot F_{R\_crp}\left(\gamma_R, t\right) \quad (1)$$

$$J_w \dot{\omega}_L = T_{tor} - r_L \cdot F_{L\_crp}\left(\gamma_L, t\right) \quad (2)$$

$$\left(m_w + \frac{m_b}{4}\right)\dot{V} = F_{R\_crp}\left(\gamma_R, t\right) + F_{L\_crp}\left(\gamma_L, t\right) \quad (3)$$

$$T_{tor} = k_s \cdot \Delta\theta_s + c_s\left(\omega_R - \omega_L\right) \quad (4)$$

where, T_e is the driving torque transmitted from the motor through a gearbox, T_{tor} is the torsional torque, $F_{R\text{-}crp}$ is the creep force at the right wheel and $F_{L\text{-}crp}$ is that at the left wheel, J_w and J_{mg} are moment of inertias of wheel and motor/gearbox respectively, m_w and m_b are wheelset and vehicle masses respectively, n is the gearbox ratio, k_s is the torsional stiffness and c_s represents the material damping of the axle, ω_R and ω_L are the angular velocity of the right and the left wheel respectively, $\Delta\theta_s$ is the relative rotation between the two wheels, γ_R and γ_L are the creepages at the right and left wheels.

The interactions with the lateral and yaw motions of the wheelset are considered in the full performance assessment, although the models are not given in the paper as they are not concerned with the control design.

3. WHEEL-RAIL CONTACT AND SYSTEM DYNAMICS

The contact forces are essential in the provision of the guidance control and the delivery of traction for railway vehicles, but can produce undesirable dynamic effects under more extreme contact conditions. When the adhesion level is high, contact forces at the wheel-rail interface are approximately a linear function of the creepages (i.e. in the low creep and linear region) and the creep coefficients are normally large. The large creep coefficients (in the order of MNs) provide a high level of damping to all dynamic motions of a wheelset, with the exception of the kinematic mode (related to the yaw and lateral modes of the wheelset) which are in practice stabilised as a part of the design for primary suspensions. In low adhesion conditions, it is much more likely that a wheelset would operate in the non-linear or even the unstable region of the slip curve, where the damping effect is significantly lower (or becomes negative).

A stability analysis to study how the wheelset dynamic behaviours are affected by different contact conditions is carried out based on the linearization of the creep - creep force curves at individual operating points. Fig. 4 shows the migration of eigenvalues with the increase of the creepage, where the two wheels are assumed to have the same creepage, the wheelset speed is 30m/s and the resonant frequency of the torsional mode is set to 60Hz. In the linear (low creep) region of the creep curve, the positive damping keeps all the modes concerned clearly stable (as indicated by '*'). However, once the creep is increased beyond the peak value (as indicated by 'o'), there are potentially two unstable modes. One is the torsional mode of the axle which is indicated by the pair of the unstable conjugate poles. The other is the common rotation of the two wheels indicated by the unstable pole on the real axis. Similar observations may be made with axles at different torsional frequency and at different speed/contact conditions [Mei et al, 2006].

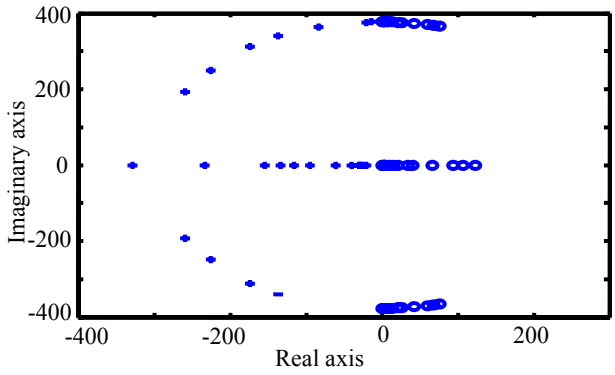

Fig. 4. Eigenvalue migrations with contact conditions (Vs=30m/s; f=60Hz; adhesion coeff=0.1)

Because the existence of sustained external disturbances to the railway vehicles, in particular those related to the track inputs, an unstable or even lightly damped wheelset would lead to potentially damaging oscillations at a frequency that is very high for a mechanical system. In the railway industry, the vibrations have been largely considered as a 'problem' that must be overcome, because they may lead to component failure or rail corrugation [Hardwood et al, 1991 and Lu et al, 1996].

However, the link between the level of damping (or stability) for the torsional mode and the wheel-rail contact conditions provides an excellent opportunity for control engineers to explore in the pursuit of alternative slip detection and anti-slip control methods. This paper will build upon the general principle of the novel slip detection that have been introduced before [Mei et al 2006 and Yu et al 2006], and present more technical detail on the control design and performance assessment.

4. CONTROL SYSTEM DESIGN AND ASSESSMENT

4.1 Slip detection with axle based sensor

If a reliable sensor can be provided to measure directly the torsional torque in the axle, the vibration signals at the resonant frequency would clearly provide an easy solution to

for detecting wheel slip. This may be achieved by the use of some fairly standard data processing techniques as shown in Fig. 5. The band pass filter can be designed to provide a narrow pass band for the frequency of the torsional mode to avoid possible interferences from other dynamic modes in the system. The low pass filter is used to remove the effect of the change of traction effort from the traction motor. The threshold will have to be carefully tuned to provide a reliable detection of wheel slip and in the meantime avoid false detection.

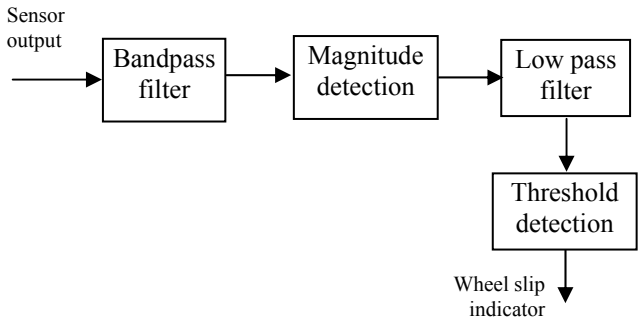

Fig. 5. Wheel slip detection with axle based sensors

Figure 6 shows how the magnitude of the torsional vibration (the output of the low pass filter) is linked to the wheel slip, where the maximum adhesion coefficient is changed from 0.4 to 0.05 at the time of 4s.

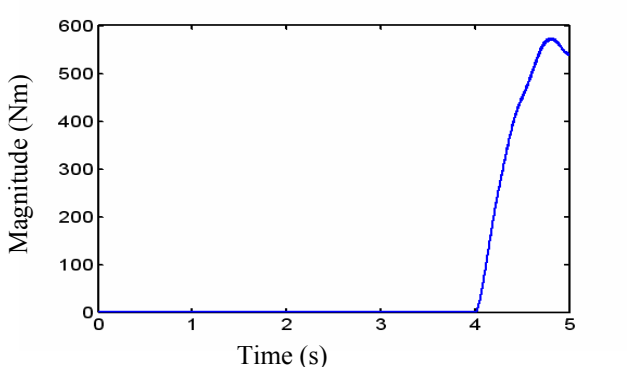

Fig. 6. Magnitude change of the torsional motion

One of the main practical challenges for this scheme would be the issue of reliable and cost effective sensing and transmission of the axle torque, because of the harsh working environment. This may become possible with recent advances in sensing technologies, e.g. a rotary torque transducer based on the so-called Surface Acoustic Wave technology (which is essentially 'frequency dependent' strain gauges to measure the change in resonant frequency caused by an applied shaft strain) is reported to offer a low cost and non-contact solution [Anon, 2001].

4.2 Slip detection with speed sensor

For practical applications, however, it is obviously desirable to minimise the use of sensors and reduce costs. In particular, the requirement of axle based vibration measurement is undesirable. In this study the measurement of the axle speed, which is normally provided in rail traction systems, is explored in the development of a Kalman filter that estimates the torsional vibrations.

To reduce the complexity of the Kalman filter, a linearised model is derived to represent the key features of the wheelset dynamics as given in equations 5 and 6.

$$\begin{bmatrix} \dot{\Delta\omega}_R \\ \dot{\Delta\omega}_L \\ \dot{\Delta\theta}_s \end{bmatrix} = \begin{bmatrix} -\frac{k_1}{J_R} & 0 & -\frac{k_s}{J_R} \\ 0 & -\frac{k_2}{J_L} & \frac{k_s}{J_L} \\ 1 & -1 & 0 \end{bmatrix} \begin{bmatrix} \Delta\omega_R \\ \Delta\omega_L \\ \Delta\theta_s \end{bmatrix} + \begin{bmatrix} \frac{1}{J_R} \\ 0 \\ 0 \end{bmatrix} \cdot \Delta T_e \quad (5)$$

$$Y = \begin{bmatrix} 1 & 0 & 0 \end{bmatrix} \cdot \begin{bmatrix} \Delta\omega_R \\ \Delta\omega_L \\ \Delta\theta_s \end{bmatrix} \quad (6)$$

where additional variables J_R ($=J_w + n^2 J_{mg}$) and J_L ($=J_w$) are moment of inertias of right and left wheels respectively, and Y represents the output measurement; and k_1 and k_2 are the rate of change on the creep-creep force curve corresponding to the creepages at the two wheels.

This is clearly a small signal model which, in a strict sense, is only valid at defined operating point(s) on a particular creep-creep force curve and therefore a Kalman filter obtained from the model should ideally only be used to provide estimations under the particular condition. It is possible to design and use a bank of Kalman filters to cover a wide range of contact conditions, but this would substantially increase the system complexity. For simplicity, a single Kalman filter is designed using the model given in eqs 5 and 6 in the proposed scheme, but the values of k_1 and k_2 are selected to focus primarily in the saturation region of the creep – creep force curves that is critical for a fast slip detection. Although a bank of filters may be used for different operating points of the creep curves, this is a compromised solution between the accuracy and simplicity of the estimations.

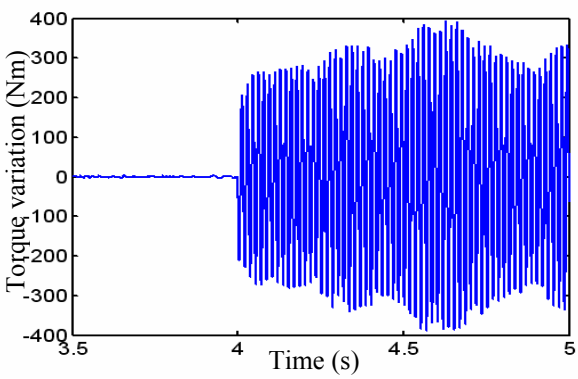

Fig. 7. Torsional motion from full simulation model

A comparison of the original and estimated torsional motions is given in Figs 7 and 8. Although a close match is not achieved in this case, the Kalman filter provides an estimation that captures the essential vibrations which is sufficient to detect the occurrence of a wheel slip.

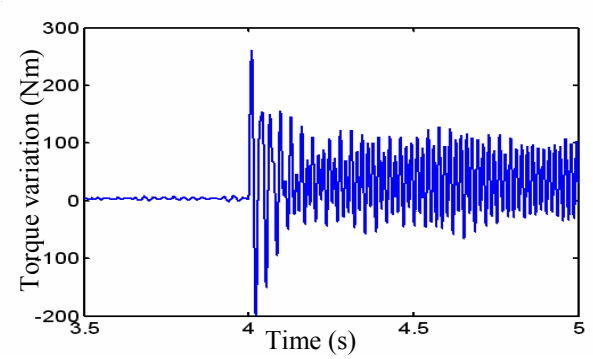

Fig. 8. Estimated torsional motion from Kalman filter

4.3 Re-adhesion control

The overall readhesion control scheme is shown in Fig. 9. The Kalman filter provides an estimation of the torsional torque of the wheelset axle from the measurement of the rotational speed of one of the wheels. An additional input of the output torque from the traction motor may also be needed, which can be provided from the motor torque controller. The output of the Kalman filter is processed to obtain the magnitude of the torsional vibrations at the resonant frequency (as shown in Fig. 6). Once a wheel slip is deemed to have occurred by the threshold detector, the torque reduction control will be switched on to reduce the torque demand below the adhesion available at the wheel-rail interface.

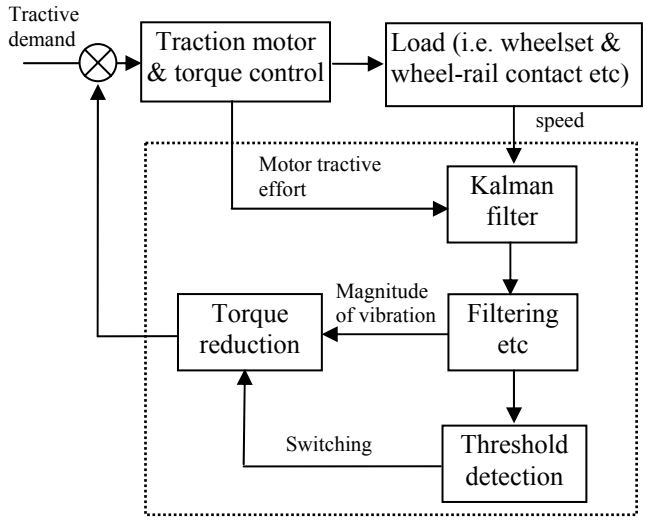

Fig. 9. Readhesion control scheme

A conventional PI controller is used and tuned to provide adequate level and speed of the torque reduction depending on the level of the magnitude of the estimated torsional torque, where the integral term is necessary to help and maintain the torque demand at an appropriate level even after a re-adhesion is achieved and there is no longer a wheel slip. A hysteresis control for the switching would help to increase/restore the original torque demand after the contact condition has improved.

4.4 Performances in different conditions

The worst case scenario for wheel slip is if there is a sudden reduction of adhesion on the track when there is a high level of tractive effort applied. Fig. 10 compares wheel and (equivalent) vehicle angular velocities during the vehicle acceleration from an initial speed of 10km/h. At the time t=4s, the adhesion of the track is reduced to well below the tractive effort, and consequently a severe wheel slip occurs and the slip ratio reaches as much as 60% in less than 0.5s before being detected. The re-adehsion control is clearly effective in reducing the torque output from the motor rapidly and the recovery time takes about 1.5s.

If the adhesion is already low when a tractive effort is applied and increased gradually, the wheel slip (when it occurs) tends to be less severe as the net torque driving on the wheelset is relatively low. On the other hand the torsional vibrations will also be smaller and less sensitive to slip conditions. However, the proposed control scheme appears to deliver a robust performance in different conditions as illustrated in Figs. 11 and 12. At the low (initial) speed of 10km/h, the peak slip ratio reaches approximately 20% and the wheel slip is quickly detected and a complete re-adhesion is achieved within a fraction of a second. At the higher speed of 100km/h, the peak slip ratio is about 14% but the recovery time takes somewhat longer as the system has to overcome a higher level of kinematic energy stored in the wheelset.

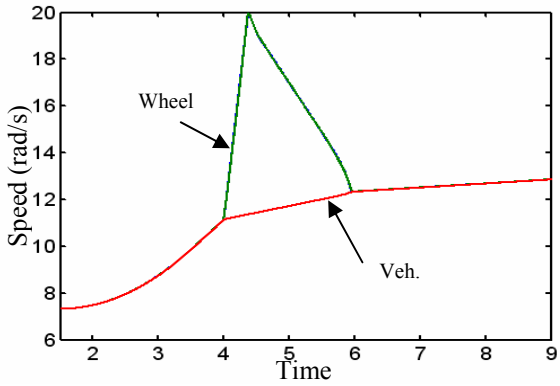

Fig. 10. Re-adhesion control – reduced adhesion at t=4s (initial vehicle speed of 10km/h)

For the wheelset with a different axle stiffness, the centre frequency of the bandpass filter used for detecting the resonant vibration of the axle must obviously be tuned to coincide with the different torsional frequency. Fig 13 shows the simulation results using a more rigid axle where the torsional frequency is changed from 60 to 80Hz. Again the detection of a wheel slip and a complete re-adhesion are achieved in less than 2s. In this, a second (smaller) wheel slip is observed which is quickly detected and eliminated by the controller – a clear evidence that the system operates very closely to the maximum adhesion region on the creep-creep force curve which is expected.

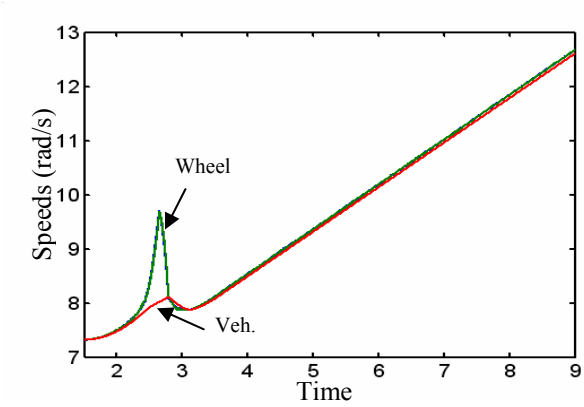

Fig. 11. Re-adhesion control – low adhesion from t=0s (initial vehicle speed of 10km/h)

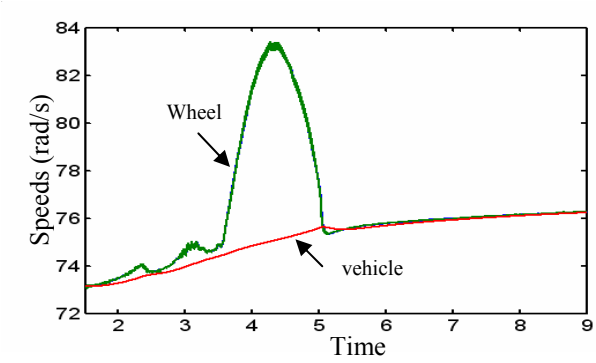

Fig. 12. Re-adhesion control – low adhesion from 0s (initial vehicle speed of 100km/h)

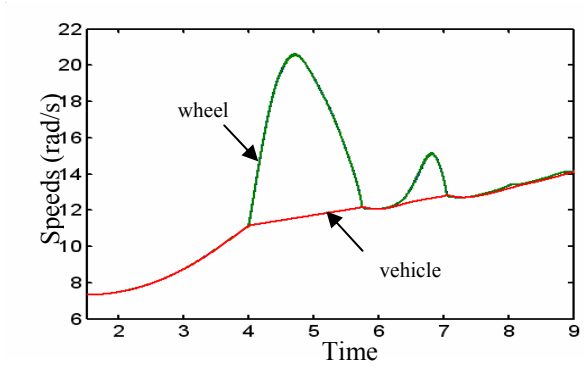

Fig. 13. Re-adhesion control – reduced adhesion at t=4s (a more rigid axle, initial vehicle speed of 10km/h

5. CONCLUSIONS

Effective use of the maximum adhesion available without causing any damaging wheel slip is an important and challenging requirement in railway traction. A new concept for the slip detection and re-adhesion control has been presented in this paper. Unlike conventional anti-slip control techniques, the new control strategy does not require the measurement of train speed or the slip ratio, which can be problematic to obtain in practice. Because the slip detection is based on the observation that the wheel slip is closely linked to the wheelset torsional vibrations, it inherently enables an optimal use of the adhesion regardless of the uncertainties/variations of the contact characteristics.

REFERENCES

Watanabe T, and Yamanaka A et al (1997), Optimisation of readhesion control of Shinkansen Trains with wheel-rail adhesion, *IEEE Power Conversion Conference (PCC'97)*.

Schwartz H J, and Krebe R (1997), Implementation of an advanced wheel creep control with searching strategy on a light rail vehicle, *European Power Electronics Conference (EPE'97)*.

Yasuoka I, and Henmi T et al (1997), Improvement of re-adhesion for commuter trains with vector control traction inverter, *IEEE Power Conversion Conference (PCC'97)*.

Park D, and Kim M S et al (2001), Hybrid re-adhesion control method for traction system of high speed railway, *IEEE Power Conversion Conference (PCC'97)*.

Kadowaki,S., Ohishi, K., Miyashita I. and Yasukawa (2002). Re-adhesion control of electric motor coach based on disturbance observer and sensor-less vector control, *Proceedings of the Power Conversion Conference,* Volume 3, p1020 – 1025.

Kim W S, Kim Y S, Kang J K and Sul S K (1999). Electro-mechanical re-adhesion control simulator for inverter-driven railway electric vehicle, *IEEE Industry Applications Conference*, Volume 2, p1026 – 1032.

Waring J R (1994), Adhesion modification tests 1993, Part 4: Centrac HPF results, *BR Research*, March, 1994, pp160.

McEwen, I J (2003) Review of the use of chemicals in the management of low adhesion, *RSSB report*, April, 2003

Mei T X, Yu J H and Wilson D A (2006), Wheelset dynamics and wheel slip detection, *STECH2006*, Chengdu, China.

Yu J H, Mei T X and Wilson D A (2006), Re-adhesion control based on wheelset dynamics in railway traction system, *UKACC2006*, Glasgow, UK

Polach O (2003), Creep forces in simulations of traction vehicle running on adhesion limit", *6th International conference on contact mechanics and wear of rail/wheel systems* (CM'2003)

Hardwood N A, and Keogh P S (1991), Self-excited oscillation in locomotive transmission systems under loss of adhesion", *Institute of Mechanical Engineers*, C414/063.

Lu G, and Harwood N A (1996), Prediction of torsional vibration on mass transit vehicle", *Computers in Railways'96*, Volume 2: Railway Technology and Environment.

Anon (2001), SAW-based transducers for non contact torque, *Electronicstalk*, 21 Feb 2001